Design of thin, high permittivity, multiband, monopole-like antennas

Mohamed Rohaim[1], Jari J J Kangas[1], Riikka Mikkonen[1], and Matti Mäntysalo[1]
[1]Electrical Engineering, Tampere University, FINLAND

We address the design of multiband monopole–like antennas on thin, flexible, and high permittivity substrates. Antennas on such materials are of interest, e.g., in IoT applications and in printable electronics. As practical example we design an antenna for three LTE bands (0.8, 1.8, 2.6 GHz with bandwidths greater than 100 MHz). The substrate used is 275 μm thick, it has $\epsilon_r \approx 11$ and low dielectric loss and it supports screen printing.

Our goals are (i) analyze step-by-step how various geometrical features affect the antenna performance and (ii) discuss building, modeling, and testing. We provide frequency domain, time domain, and characteristic mode analyses and measurement results.

***Index Terms*—Monopole–like antennas, antenna design, thin flexible substrate, screen printing, characteristic modes.**

I. Introduction

Antennas are needed in various wearable and IoT applications where e.g. compact size, light weight, and ease of mass production are of interest. For such applications e.g. thin and flexible materials and alternative construction techniques such as printable electronics are of interest.

We design a thin high permittivity monopole–like antenna (see Fig. 1) and aim to add new insights about the working principles of such antennas. Section II lists preliminaries, section III presents simulation results of various factors that affect the antenna performance, and section IV discusses test results and testing this type of antennas and gives conclusions.

II. Preliminaries

A. Application requirements and previous works

Our practical design example is a multiband antenna for a wireless sensor sticker application. The antenna should work at three LTE bands (0.8, 1.8, 2.6 GHz) with bandwidths (BW) greater than 100 MHz ($S_{11} < -10$ dB). The antenna should be linearly polarized and have gain reaching close to 2.0 dBi. The antenna and application circuitry are aimed to be integrated on the same thin substrate. Due to the thin substrate, monopole–type design was chosen, e.g. instead of patch–type design. The monopole arm and a microstrip feed line are on the same side of the dielectric substrate and a ground plane is on the other side, see Fig. 1.

Literature includes many different monopole–type designs to obtain dual-band or multi-band antennas. The suggested antenna geometries have had different shapes e.g. T-, G, F, to obtain the desired dual-band, tri-band or multi-band performance [1]–[5]. We propose a compact tri-band antenna and combine characteristic mode analysis and time domain analysis to carefully analyze factors affecting the antenna performance. A recipe to design such antennas is given.

B. Antenna screen printing

Test antenna patterns were screen-printed (TIC SCF-300 printing machine) on a thin flexible substrate (PREPERM®TP20556, dielectric constant $\epsilon_r \approx 11$, dielectric loss ≈0.001, thickness 275 μm). Screen printing allows low resistance conductive patterns as it offers thicker layers (10–20 μm) than other printing technologies (typically 0.5–2 μm). We used screen ink (Novacentrix HPS-021LV) containing silver flakes (70–80%), water (10%) and organic solvents, due to reported excellent electrical (DC) properties [6]. A polyester mesh screen was used in the printer. The mesh was attached to a 500×3000 mm^2 aluminum frame with a profile of 30×30 mm^2. The mesh count was 79 threads/cm, mesh opening 81 μm, and stretching angle of the mesh 22.5°.

First, antenna top sides were printed and oven-cured. Then, holes were drilled for the via connecting antenna top side to the ground plane. Additional holes were drilled in line with the first hole to align the ground when the non-transparent substrate was turned around for the second printing round. Antenna grounds were printed on the other side of the substrates to finish antenna layout. Prints were again cured in the oven. DC sheet resistance was measured from antenna ground planes using a four-point probe station. Sheet resistances of 29 mΩ/□ were acquired which agree with measured line thicknesses (15 μm in average).

C. Simulation methods and their settings

In simulations we used frequency domain (FDA: ADS 2016.1), time domain (TDA: CST 2018.00), and characteristic mode analysis (CMA: CST multilayer solver). Only lossless substrate and perfect electric conductors are supported by the CMA on CST (causing e.g. a minor shift in the resonance frequencies compared to TDA).

CMA calculates excitation independent characteristic modes (modal currents, eigenvalues, modal radiated fields) i.e. a set of (orthogonal) current modes supported by the structure. The response of an excitation driven antenna at a certain frequency is a combination of these modes at the frequency [7].

For FDA and TDA the antennas are excited by a discrete port through a 10 mm segment microstrip feedline of width = 250 μm which results impedance of 47.6 Ω. The width was due to screen printing technology limitation. For conductors, $\sigma = 5e6$ S/m was used. The feed point is shown in Fig. 1. The simulated antennas lie on the xy-plane, y-axis and $\phi =$

Manuscript modified January 15, 2021. Corresponding author: J. Kangas (email: jari.kangas@tuni.fi).

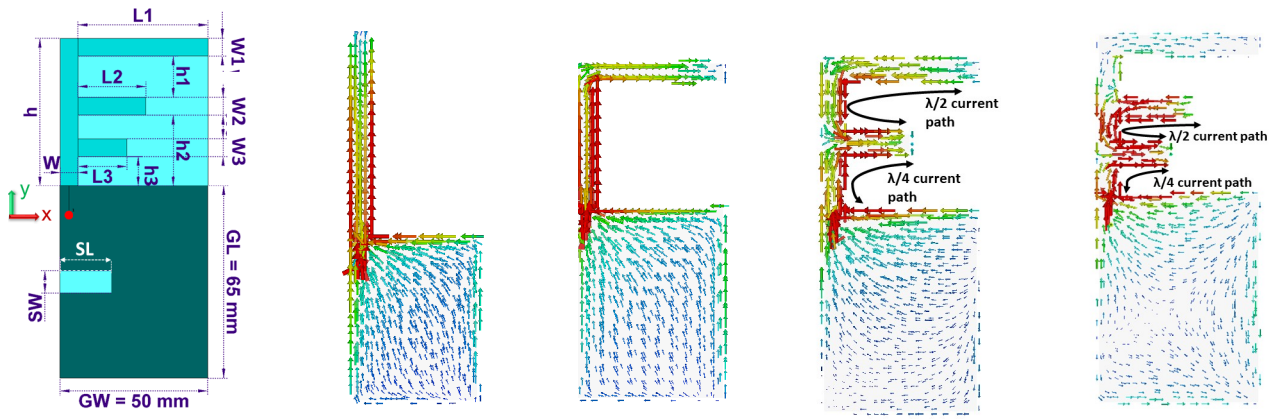

Fig. 1. Dimensional parameters and feed point location (red circle), dark turquoise depicts ground. Surface current distributions (TDA, logarithmic scale 0–15 A/m): A1 at 0.8 GHz, A3 at 0.8 GHz, A4 at 1.8 GHz, and A5 at 2.6 GHz, resp.

90°–axis are aligned, see Fig. 1. Gains are given at the design frequencies, at the direction of maximum radiation.

III. Recipe of a Multiband Antenna: Factors Affecting the Performance

We outline a recipe for the proposed antenna design and proceed step-by-step to analyze e.g. how widths of the conducting traces, widening the traces on either end, features to support multiple frequencies, and ground plane geometry affect the antenna performance. Models studied are labeled sequentially, A1, A2, …. Fig. 1 shows parameterized model and Table I nominal parameter values for each model. For all models W=6, GW=50, and GL=65 mm, their selection is discussed later. Feed point is marked as red spot in Fig. 1. Most model geometries can be deduced from Fig. 1 e.g. the ground plane slit is present only at the final 3–band designs. We simulated with substrate heights upto 1 mm and noticed no clear impact on antenna parameters. Due to application requirements we continued with fixed thickness of 275 μm.

A. 1–band, 800 MHz printed monopole antenna (A1)

The monopole (A1) dimensions are optimized for resonance at 800 MHz. With a method given in [8] the effective permittivity of our antenna structure ($\epsilon_{\text{eff}} \approx 1.15$) and thus the resonant dimensions can be estimated. Fig. 1 shows a quarter-wave surface current distribution over A1 at 800 MHz, in ground plane current is confined to the edges. CMA shows that A1 has a clear dominant mode at 800 MHz (other modes have low MS at 800 MHz) and a typical doughnut–like radiation pattern. The antenna radiates linearly polarized waves. Table II lists key antenna parameters.

B. Antenna width and ground plane dimensions

For wire monopole antennas resonance frequency decreases with thicker wire radius [9]. For A1 the resonance frequency of the dominant mode is increasing as the width (W=3,6,9 mm) increases, see Fig. 2. The CMA surface current of the dominant mode at 800 MHz suggested higher current as the antenna width increase, which could explain why input impedance curve on Smith chart (SC) shift towards low impedance. Also, MS results suggest that potential bandwidth increases as W increases (similar results given in [1]). TDA suggests the same, but matching and BW degrades as W increases too much, see Fig. 2. Thus $W = 6$ mm was chosen.

TABLE I
Nominal dimensions (unit [mm]) of studied antenna models .

Label	h	$h1$	$L1$	$W1$	$h2$	$L2$	$W2$	$h3$	$L3$	$W3$	SL	SW
A1	85	0	0	0	0	0	0	0	0	0	0	0
A2	60	0	37	0	0	0	0	0	0	0	0	0
A3	50	0	44	0	0	0	0	0	0	0	0	0
A4	50	18	44	6	20	22	6	0	0	0	0	0
A5	50	14	44	6	24	22	6	10	16	6	0	0
A6	50	14	44	6	24	23	6	10	16.5	6	17.5	7.5
A7	50	14	44	6	24	23	6	14	16.5	6	17.5	7.5

TABLE II
Simulated antenna parameters (TDA).

Label	Band (GHz)	S_{11} BW (MHz)	Gain (dBi)	Efficiency
A1	0.8	130	1.72	93.3
A2	0.8	124	1.56	93
A3	0.8	110	1.53	93
A4	0.8	113	1.53	93
	1.8	112	3.56	92
A5	0.8	110	1.63	95
	1.8	166	3.57	93
	2.6	90	3.54	82

Increasing the ground plane width GW of A1 decreased the resonance frequency (similar results given in [1]). Input impedance on SC decreased and BW increased slightly as GW increases. Decreasing GW decreases length of the current path and frequency increases, decreasing GW also shifts input impedance curve on SC away from the center towards high capacitive region which consequently decreases BW. Increasing the ground plane length GL decreases the resonance frequency and also enhances matching and BW. Considering size constraints and antenna characteristics, GW=50 and GL=65 mm yields an acceptable compromise.

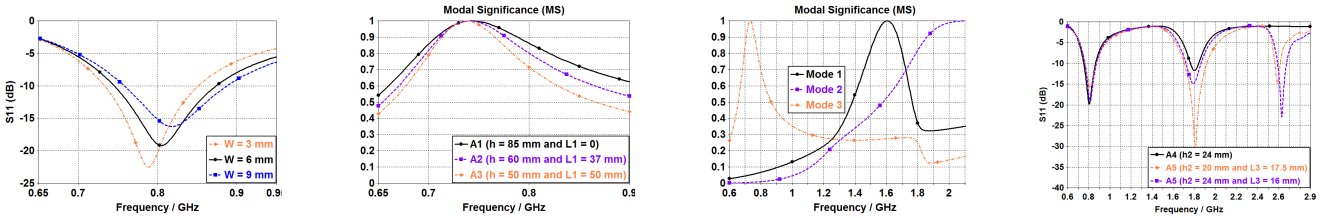

Fig. 2. (a) S_{11} of A1 when W is varied. (b) MS of A1, A2, and A3. (c) MS of A4. (d) S_{11} of A4 and A5 when $h2$ varied.

C. L-shape monopole arm (compact antenna)

Next, two L-shaped antennas resonant at 800 MHz (models A2 and A3) are studied. Their nominal dimensions are given in table I ($L1 \neq 0$ but 2nd and 3rd strips are not present). Fig. 1 shows a quarter-wave surface current distribution over A3 at 800 MHz and Fig. 2 MS of A1, A2, and A3. Input impedance circles of A1, A2, and A3 get bigger on SC as h decreases ($L1$ adjusted to keep the resonance at 800 MHz). BW decreased as h decreases as a cost for achieving size reduction.

Wider feed point width (W=3,6,9 mm) for A3 increases the resonance frequency as input resistance decreases and input reactance gets more capacitive. Wider end of the line width ($W1$=3,6,9 mm) decreases the resonance frequency as input resistance increases and input reactance gets less capacitive.

Wider $W1$ decreases the current path which should increase the resonance frequency, however, simulations showed that the resonance frequency decreased (similar results given in [1]). Increasing the width near the radiating edge increases the fringing fields which, consequently, increases the effective length of the antenna and the resonance frequency decreases. Impact of the width near the feed point is more dominant.

D. Tri-band antenna, Adding second and third strips

Second horizontal strip added to A3 (model A4) creates resonant frequency at the 1.8 GHz band. Fig. 1 shows current distribution on A4 at 1.8 GHz. MS of A4 around 1.8 GHz show a clear dominant mode due to the 2nd strip whilst 800-MHz resonance mode has low MS, see Fig. 2. A higher order mode (2.4 GHz) has high MS at 1.8 GHz but small current near the feed point, so it is not excited by our feed setup. Antenna parameters of A4 are given in Table II.

The second horizontal strip creates resonance path (λ/4 current distribution) from the feed point to the second horizontal strip open end ($h2 + L2$) and it will mainly control the new resonance frequency, as is reported also in [1] and [5]. Our simulations showed also that the 2nd horizontal forms λ/2 current path from the second horizontal strip open end to the first horizontal strip open end ($L2 + h1 + L1$), see Fig. 1.

Shifting the second horizontal strip up ($h2 : 20 \rightarrow 24$ mm) degrades matching and BW. This happens as the λ/2 current path ($L2 + h1 + L1$) and the λ/4 current path ($h2 + L2$) do not occur around the same frequency any more. Shifting the second horizontal strip down ($h2 : 20 \rightarrow 12$ mm) enhanced input impedance and BW. Shifting the second horizontal strip down made the λ/2 current path ($L2 + h1 + L1$) and the λ/4 current path ($h2 + L2$) occur closer to the same frequency. As a guideline, one can start from $L2 + h1 + L1 = 2 * (h2 + L2)$, but the best performance is obtained when $L2 + h1 + L1 > 2 * (h2 + L2)$. Thus; fixing h and $L1$, input impedance at 1.8 GHz can be controlled by tuning $h1$ and $h2$, while the resonance frequency can be tuned by varying $L2$. However, $h2$ cannot be too small as it affects the results of the 2.6 GHz band as is explained later. The 2nd strip does not affect results of the 800 MHz band. Increasing the ground plane length GL enhances matching and BW of the 1.8 GHz band.

Third horizontal strip (model A5) creates additionally the 2.6 GHz band, see Fig. 2. The working principle is as for A4 in the 1.8 GHz band. The 3rd strip creates third resonant path which forms (i) λ/4 current distribution from the feed point to the third horizontal strip open end ($h3 + L3$); and (ii) λ/2 current distribution from the third horizontal strip open end to the second horizontal strip (1.8 GHz arm) open end (L3 + h2 + L2). The first strip is not effective at the 2.6 GHz band as it has small amount of surface current (Fig. 1) and S_{11} of A5 shows three bands (Fig. 2).

It holds that $L3$ mainly controls the resonance frequency, while $h3$ and $h2$ control the input impedance and BW of the 2.6 GHz band. The input impedance and BW of the 2.6 GHz band are enhanced by shifting the second horizontal strip up ($h2 : 20 \rightarrow 24$ mm, $L3$ adjusted to keep resonance frequency). Results of the 1.8 GHz band were also enhanced noticeably by the third horizontal strip which is due to couplings between 2nd and 3rd strips (similar results given in [2]). We also varied $W2$ and $W3$ to optimize results, but decided to continue in the paper with $W2$=$W3$=6 mm for simplicity.

A5 has four modes with high enough MS to affect the 2.6 GHz band. The excitation setup can support modes 1 and 4 but modes 2 and 3 should be suppressed as they have small current near the feed point. Mode 4 (at 2.6 GHz) has 2 lobes with end-fire radiation which affected the overall pattern at 2.6 GHz and thus we wanted to suppress mode 4 which has current distribution confined to the edges of the ground plane. In [10], the effective current path in ground plane was increased by adding four slots. Thus we introduced a narrow slit in the ground plane (model A6) to shift resonance frequency of mode 4 down by increasing length of its current path. Position of the slit was determined based on the surface current distributions of modes 1 and 4 and its dimensions SL and SW were tuned to shift mode 4 down to around 2 GHz (not lower to affect the 1.8 GHz band). Fig. 3 shows MS of modes 1 and 4 with and without the slit. With the slit mode 4 has lower MS and also antenna radiation pattern is more broadside. Fig. 3 shows radiation pattern of A6 at the yz-plane. The ground plane

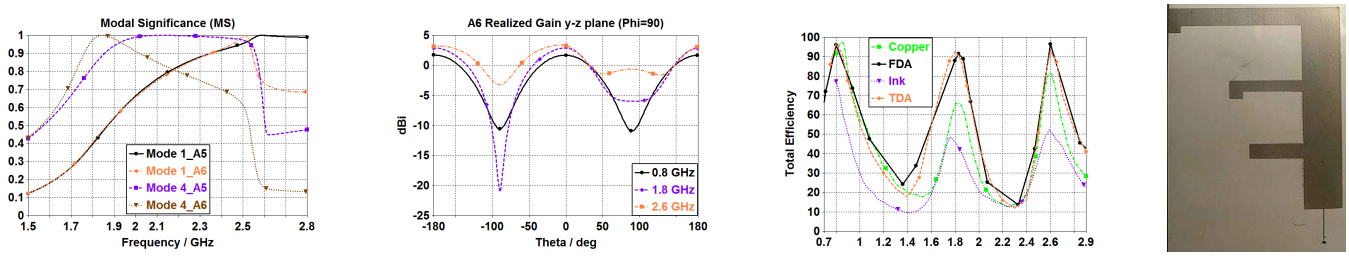

Fig. 3. (a) MS of modes 1 & 4 supported by the feed setup. (b) Radiation pattern of A6 [dBi]. (c) Simulated and measured efficiencies. (d) Ink–printed prototype arm.

slit affects the resonance frequencies of the 1.8 and 2.6 GHz bands, thus model A6 has $L2$=23 mm and $L3$=16.5 mm. Table III shows (TDA) antenna parameters of A6.

IV. Prototype antennas

Several prototype antennas with conducting traces made either via screen printing or from copper tape were built and tested We show result for a prototype whose dimensions resemble A6 (h was 56 mm instead of 50 mm). Fig. 3 shows an ink–printed prototype arm, we tested also adding hooks at the end of the strips to enhance BW and to reduce the antenna size, but had to exclude study about their effects from the paper. Overall, measurements and TDA results matched well and thus only part of the measurement results are included.

A. Testing prototype antennas

A VNA was used to measure antenna S–parameters and an antenna test chamber (StarLab, Satimo) for other antenna parameters. Most antennas had SMA connector either soldered to copper tape or glued (with conductive glue) to the printed traces. We tested if the SMA connector affected measurements and had one prototype with about 10 cm long coaxial line probe (50 Ω UT-085C with female SMA at the other end). The probe was soldered on the bottom side of the ground plane. No significant differences were noticed between the cases. The thin substrate allows bending the antenna, but that was not tested in detail.

Table III and Fig. 3 show FDA, TDA, and measurement results, the design fulfills the specifications except the ink version has lower gain and efficiency. Moreover, the ink version did not meet the BW–criteria (in worst case it had 100 MHz BW with $S_{11} < -6$ dB). One possible issue is the narrow feed line whose width was at the limit of the screen printing technology used. Most likely its realized impedance differed from 50 Ω. The recipe was successfully extended to design a 4–band antenna (model A7 in Table I, for 4th arm $h4$=3, $L4$=6.5, $W4$=5 mm) which had 4th band at 5.2 GHz (BW 500 MHz, max gain 5.0 dBi).

B. Conclusions

We presented a recipe to design monopole–like multiband antennas and used it successfully to design a tri-band compact printed monopole antenna on a thin substrate.

Our study provides understanding on the working principles of this type of antennas, esp. combination of the CMA and other techniques allowed a route for a systematic antenna design approach. Use of thin substrate had challenges, but its flexibility is of importance in many applications. The slit on the ground plane suppressed unwanted mode(s), but slit(s) may be unwanted for building circuitry on the bottom side of the ground.

TABLE III
Simulation and measurement results

Band (GHz)	Type	S_{11} BW (MHz)	Gain (dBi)	Efficiency
0.8	TDA	110	1.87	0.96
	Copper tape	120	2.54	0.91
	Ink	–	1.27	0.65
1.8	TDA	130	2.47	0.78
	Copper tape	105	2.14	0.65
	Ink	–	1.31	0.42
2.6	TDA	100	4.1	0.88
	Copper tape	115	4.32	0.81
	Ink	–	3.48	0.46

References

[1] Y.-L. Kuo and K.-L. Wong, "Printed double-T monopole antenna for 2.4/5.2 ghz dual-band wlan operations," *IEEE Transactions on Antennas and Propagation*, vol. 51, no. 9, pp. 2187–2192, 2003.

[2] H. Zhai, Z. Ma, Y. Han, and C. Liang, "A compact printed antenna for triple-band wlan/wimax applications," *IEEE Antennas and Wireless Propagation Letters*, vol. 12, pp. 65–68, 2013.

[3] C.-Y. Pan, C.-H. Huang, and T.-S. Horng, "A new printed G-shaped monopole antenna for dual-band wlan applications," *Microwave and Optical Technology Letters*, vol. 45, no. 4, pp. 295–297, 2005.

[4] H. F. Abutarboush and A. Shamim, "Paper–based inkjet-printed tri-band u-slot monopole antenna for wireless applications," *IEEE Antennas and Wireless Propagation Letters*, vol. 11, pp. 1234–1237, 2012.

[5] S.-H. Yeh and K.-L. Wong, "Integrated F-shaped monopole antenna for 2.4/5.2 ghz dual-band operation," *Microwave and optical technology letters*, vol. 34, no. 1, pp. 24–26, 2002.

[6] R. Mikkonen and M. Mäntysalo, "Evaluation of screen printed silver trace performance and long-term reliability," *Microelectronics Reliability*, vol. 86, pp. 54–65, 2018.

[7] M. Cabedo-Fabres, E. Antonino-Daviu, A. Valero-Nogueira, and M. F. Bataller, "The theory of characteristic modes revisited: A contribution to the design of antennas for modern applications," *IEEE Antennas and Propagation Magazine*, vol. 49, no. 5, pp. 52–68, 2007.

[8] Z. Živković, A. Šarolić, and V. Roje, "Effects of effective dielectric constant of printed short dipoles in electric field probes," in *10th International Symposium on Electromagnetic Compatibility*. IEEE, 2011, pp. 73–78.

[9] W. L. Stutzman and G. A. Thiele, *Antenna theory and design*. John Wiley & Sons, 2012.

[10] L. Zhang, K. Y. See, and Y. P. Zhang, "Impact of pcb ground plane size on dual-band antenna performance," in *2012 Asia-Pacific Symposium on Electromagnetic Compatibility*. IEEE, 2012, pp. 593–596.